EXPERT REVIEWS

Biological effects of dynamic shear stress in cardiovascular pathologies and devices

Expert Rev. Med. Devices 5(2), 167–181 (2008)

Gaurav Girdhar and Danny Bluestein†

†*Author for correspondence*
Department of Biomedical Engineering, State University of New York at Stony Brook, Stony Brook, NY 11794-8181, USA
Tel.: +1 631 444 1259
Fax: +1 631 444 6646
danny.bluestein@sunysb.edu

Altered and highly dynamic shear stress conditions have been implicated in endothelial dysfunction leading to cardiovascular disease, and in thromboembolic complications in prosthetic cardiovascular devices. In addition to vascular damage, the pathological flow patterns characterizing cardiovascular pathologies and blood flow in prosthetic devices induce shear activation and damage to blood constituents. Investigation of the specific and accentuated effects of such flow-induced perturbations on individual cell-types *in vitro* is critical for the optimization of device design, whereby specific design modifications can be made to minimize such perturbations. Such effects are also critical in understanding the development of cardiovascular disease. This review addresses limitations to replicate such dynamic flow conditions *in vitro* and also introduces the idea of modified *in vitro* devices, one of which is developed in the authors' laboratory, with dynamic capabilities to investigate the aforementioned effects in greater detail.

KEYWORDS: cardiovascular disease • cone-plate viscometers • dynamic shear stress • platelet activation • prosthetic heart valves • turbulence

Implantable blood recirculation devices, artificial hearts and heart valves, have long been used as life-saving alternatives for people with severe cardiovascular diseases. However, such devices require complex anticoagulation therapy and, as a consequence, are linked to post-implant complications, such as hemorrhage. Despite the anticoagulation therapy, the risk for cardioembolic stroke is not eliminated. Although biocompatibility of these recirculation devices is of utmost importance, optimizing the geometric design of these devices is also critical to avoid flow-induced trauma to blood. Over the years, a definite link between fluid shear-stress-induced damage and activation of blood constituents such as platelets and red blood cells, has been established. Irregular flow patterns arising around complex geometries (e.g., the hinge regions of mechanical heart valves [MHV]) have been recently characterized by numerical calculations and noninvasive flow measurements, and are implicated in causing flow-induced thromboembolism (TE). For instance, the Medtronic Parallel™ valve exhibited regions of elevated turbulent stress around the hinges due to its specific geometry, which, in addition to other factors, such as localized vortex flow regions, may have led to thrombus formation in several valve recipients [1]. In another case, tilting of the valve (i.e., improper orientation during implantation) was found to cause regions of high turbulence and regurgitation flow around the implantation [2,3]. Flow-induced platelet activation within a left ventricular assist device (LVAD) due to flow past prosthetic heart valves (PHV) have also been investigated *in vitro* and *in vivo* [4–6]. However, these investigations mostly provide a bulk measure of platelet activation and it is difficult to identify the specific regions in which platelet activation occurs. In order to achieve successful and efficient device design optimization process, there is a need for *in vitro* systems that can replicate specific flow irregularities (due to device geometry) that cause the maximum thrombogenic damage.

Recent computational studies on flow-through PHVs have focused on delineating complex dynamic shear-stress trajectories during

 10.1586/17434440.5.2.167 ISSN 1743-4440

forward and leakage (regurgitation) flows upon valve closure, which has been demonstrated to have a higher propensity to cause blood damage [7–9]. Flow patterns near the hinge regions and boundary walls of PHVs induce recirculation zones and shed vortices that enhance platelet activation and promote thrombus formation, due to a combination of longer exposure times to elevated shear stresses [10]. Minor design modifications (e.g., the hinge region) in PHV manifest in varying spatio-temporal patterns of shear stress and exposure to them, and may lead to pronounced differences in platelet activation, and hence the thrombogenic performance of the valve [11]. Load history (cumulative shear stress and exposure time over Lagrangian trajectories) computed numerically and as measured by particle image velocimetry (PIV) demonstrate good correlation in both the recirculation (leakage) and jet (forward flow) zone [10,12]. Specific trajectories within the flow field, through the device, increase the rate of thrombin generation by platelets, as compared to bulk-flow trajectories. Stress-specific effects on blood therefore, need to be identified and investigated, to facilitate the modification of geometric features in the device that induce such flow pathologies.

To achieve this objective, it is essential to integrate numerical and experimental approaches in a top-down manner to estimate thrombogenic risk associated with a specific geometry of the recirculation or an implantable device. Such an approach should involve a numerical characterization of flow patterns and regional shear-stress distributions along pertinent flow trajectories within a device. This information could then be programmed into a dynamic *in vitro* shear device in which individual shear-stress patterns and their load history are replicated. The fluid of interest could be a platelet or red cell suspension or whole blood, and the damage or activation on the same due to a specific shear-stress trajectory could therefore be experimentally quantified. Effects of localized high or low shear stress may be dramatically different in their effects on circulating blood cells and the vasculature. The dynamic *in vitro* device should therefore additionally facilitate investigation of thrombogenic effects in a multicellular milieu. Most of these devices are designed to uniformly expose a suspension of cells to the same stress level, accentuating the effects of this exposure that may otherwise be masked when measuring bulk properties in a device.

The present review article discusses the importance of such regional and complex shear stresses and the *in vitro* devices that can be used to investigate their effects on cells. The development of annular and cone-plate viscometers, as compact flow systems to study laminar as well as turbulent flow, is discussed. These ideas are integrated into the hemodynamic shear device (HSD) developed in the authors' laboratory, to study shear stress-induced regulating or damaging effects on blood and the vasculature. Finally, the effect of pathological shear stresses investigated in such devices on red blood cells (RBC), platelets and endothelial cells are reviewed.

Criteria for a viscometer or HSD design

The design of the viscometer or HSD incorporates two aims:

- The ability to be a virtual and universal (device independent) thrombogenicity testing tool for any blood recirculation device for its design optimization. In other words, it should be capable of accentuating the minute effects of device design modifications (e.g., PHV pivot designs or opening angles) on the cells of interest (e.g., platelets, RBC and endothelial cells);
- The ability to investigate normal and pathological shear-stress conditions for multicellular environments, within the same device.

To accomplish these aims, the viscometer or HSD should incorporate the following features:

- The cells (suspension or cultured or both) within the viscometer should be uniformly exposed to the programmed dynamic shear stresses. Additionally, secondary flow effects in the HSD should have negligible effects;
- The viscometer should be capable of being programmed and should replicate any type of stress-loading waveforms (obtained numerically or from *in vivo* studies);
- The fluid-inertial effects within the viscometer should be negligible. In other words, the timescale over which uniformity of shear stresses is achieved should be less than that of the dynamically changing shear stresses;
- The HSD or viscometer surfaces must minimize contact activation or damage of cell suspensions. This may be achieved by utilizing approved biocompatible coatings or materials for cardiovascular devices, within the HSD;
- The viscometer must facilitate periodic sampling of cell suspensions or alternative methods such as microscopy, to monitor changes in real-time activation state of the cells, as they are being exposed to dynamic shear stress.

The following section discusses some of the key features of Couette and cone-and-plate viscometers, and their suitability for objectives mentioned previously.

Annular Couette viscometers

Background

These viscometers consist of two coaxial cylinders with the fluid of interest occupying the gap between the two cylinders. Shear stress is introduced by rotation of either cylinder, or co- or counter-rotation of both cylinders depending on the application of use. Viscosity of the test fluid as a function of shear stress, geometry and rotation rate can then be determined with empirical formulae for Newtonian fluids. The earliest rotational viscometers were designed and used to determine altered blood viscosity during pathological conditions, such as coronary occlusion and arterial thrombosis, and RBC aggregation,

under different low shear rates [13–15]. Computer-controlled Couette viscometers were introduced in the early 1980s to investigate change in viscosity of blood with increasing shear rates [16,17], and also to investigate abrupt critical shear stress and exposure time limits that induce hemolysis of RBC [18]. While mostly restricted to clinical applications (measurement of blood viscosity), *in vitro* studies investigating platelet activation and the influence of RBC on the same further led to the development of oscillatory-flow and optically transparent Couette viscometers by which flow patterns and interaction between the blood constituents could be observed under physiological conditions [16,19–23]. However, the utility of such viscometers to explore pathophysiological and device-induced dynamic shear stress conditions has only recently been implemented [24].

In order to explore highly variable shear stress effects on circulating cells, the flow field in such viscometers needs to be characterized. The primary requirement of an ideal viscometer, as mentioned previously, is to be able to maintain uniformity in shear stress over a dynamic range. Secondary flow effects such as the formation of turbulent eddies, vortices and other regions of localized shear stress, may induce artifactual effects on the cells. For instance, the Kolmogorov length scale for the smallest eddy for flow past MHV was found to be 4.66 µm [6]. This being comparable to the diameter of the platelet (~1.5–4 µm) poses a high risk of localized strain on the platelet membrane, and subsequent activation. The level of tolerance to secondary flow or turbulence therefore may depend on the size and the mechanical or structural properties of cells. For instance, RBC are much more resistant to damage relative to platelets and require an order of magnitude higher stress to induce such effects [25–28]. An example of such a secondary flow pattern in the form of Taylor vortices in Couette viscometers is discussed in the following section.

Taylor number & annular flow

In annular Couette flow, a dimensionless parameter called the Taylor number determines the importance of centrifugal or inertial forces relative to viscous forces, for the problem of interest. The inertial forces have a tendency to destabilize the viscous forces and lead to instabilities called Taylor vortices [29]. In the special case of stationary outer and rotating inner cylinder, the Taylor number may be defined as:

$$T = \frac{2R_i^2\delta^4}{R_0^2 - R_i^2}\left(\frac{\omega}{\upsilon}\right)^2 \quad (1)$$

where R_0 is the outer cylinder radius, R_i is the inner cylinder radius, ω is the rotational velocity of the inner cylinder, δ is the annular gap width and ν is the kinematic viscosity of the fluid of interest [30]. The formation of Taylor vortices due to secondary flows between the gap or clearance between two coaxial cylinders (rotating inner and stationary outer) have been extensively investigated [31,32]. Such vortical flow patterns have been recently utilized to predict their effects on platelets (e.g., increased residence time and higher mixing, possibly leading to more thrombin generation and platelet activation). They have been speculated to decrease contact between the platelets and the artificial surface (of the device or viscometer) and reduce activation (Platelet Factor-4 release) compared with laminar steady flow [33].

For the narrow gap limit (radius ratio $\rightarrow$ 1), the Taylor number may be approximated as [18,34]:

$$T = R_i\delta^3\left(\frac{\omega}{\upsilon}\right)^2 = R_e^2\frac{\delta}{R_i} \quad (2)$$

where R_e is the Reynolds number and other parameters are as defined above. The critical Taylor number for the onset of secondary flow (or Taylor vortices) has been reported to be Tc = 1712 for water [35]. In problems with highly dynamic shear stresses where T is likely to exceed Tc, investigation of timescale for change in Taylor number and onset of secondary flow becomes important. It was recently demonstrated with linear stability analysis of Couette flow in the narrow annular gap limit (assuming infinite cylinders) that the time of onset of secondary flow depends on the Taylor number as [34]:

$$\tau_c = 20.05T^{-2/3} \quad (3)$$

The time limit when secondary flow is clearly observed is approximately $4\tau_c$ and supports experimental data [36]. The timescales for onset of such transient dynamic instabilities (<0.2 s) may be nearly instantaneous while investigating dynamic shear stress patterns within *in vitro* experiments. Highly complex flow behavior has been reported for annular Couette flows depending on radius and aspect (ratio of gap width to cylindrical height) ratios [37,38], Reynolds number and dynamics of rotation, such as transitions from circular Couette to Taylor Couette to wavy vortex to turbulent vortex flow [39]. Dynamics of such flow effects can be predicted numerically and explain the enhanced platelet activation in regions of complex flow with relatively smaller Reynolds numbers, but with presumably higher exposure times and collision frequencies.

Design optimization of Couette viscometers

It is critical to identify parameters to minimize development of vortices and reverse-flow regions, in order to study the effect of uniform shear stress on a cell suspension. As mentioned previously, development of vortical flow depends strongly on the annular gap width and is inversely correlated to the radii [18]. Such vortices may either originate from the end walls (outer cylinder) and propagate inwards [38], or conversely, and may manifest other forms of instabilities [40], in the narrow gap limit. Once developed, the limits of stability of such modes or patterns of flow may be determined with explicit formulae [32]. A recent blood shearing instrument (BSI) design methodology based on Couette flow utilized CFD simulations for various annular gaps and rotational speeds, and reported that uniformity of shear stress depends on the absolute magnitude of the gap and the ratio of circumferential and axial Reynolds stresses. For a small gap and optimized geometry, uniformity

in shear stress (up to 1500 Pa) and minimization of vortices and flow reversal may be achieved [41]. A similar approach could be adopted to optimally design the Couette region of a viscometer device.

Thus, the system of coaxial cylinders with limiting annular gap and with the inner rotating cylinder may be utilized to investigate shear induced platelet activation (SIPA) under dynamic conditions, such that the Taylor number does not exceed the critical value. However, this configuration may not be suitable for investigating SIPA in the presence of endothelial cells (ECs) or cultured cells, which may be difficult to culture on curvilinear annular regions of the cylinders. The cone-plate viscometer may therefore be much better suited for multicellular environments involving both cultured and circulating cells.

Cone & plate viscometers

Background

Introduced in 1934 by Mooney and Ewart [42], it was later used as an alternative to the coaxial Couette viscometers to measure viscosity of biological fluids [43]. The cone and plate viscometer (CPV) has been extensively used since the early 1980s to measure platelet activation, blood viscosity and RBC damage (hemolysis) [44–46]. The CPV consists of a rotating cone on top of a flat base-plate, with the fluid of interest between the conical surface and the base-plate. The angular separation between the cone surface and the base-plate is typically 0.5°–3°, to maintain uniform shear stress on the fluid of interest (independent of the radial location and the gap clearance). The rotation of the cone can be dynamically controlled with a motor connected to a programmable interface [24,47]. Recently a dynamically controlled CPV system (DFS) proposed by Blackman and colleagues overcame the limitations of handling complex shear-stress patterns [24,48]. The system is readily programmable and reproduces arterial shear-stress waveforms as accurately as 0.02%, the lag due to the inertial effects of the system being minimal (~0.01 s). In their recent work, the group used typical-atheroprone and atheroprotective waveforms obtained from imaging studies on the left carotid human artery, to show that phenotypical differences in ECs arise when cultured under these two distinct conditions [49]. The system is mounted on top of an inverted microscope and real-time microscopy of changes in the cells is thus facilitated. More recent applications thus include the effect of shear stress on mechanotransduction and morphological response of ECs [49,50], the interaction between platelets and ECs or ligand coated surfaces [51,52], and the interaction between platelets and RBC in pathology [53].

Optimal design of the cone-plate system is essential for studies involving higher shear stresses. Nondimensional Womersley and Reynolds numbers may be used to determine whether secondary flow effects due to dynamic or oscillatory flow conditions become highly significant [54,55]. Such regional effects are interdependent functions of sample volume, cone angle, cone radius and shear rates [55]. A single modified Reynolds number (discussed in the following section) of the form:

$$\tilde{\mathrm{Re}} = (r^2\omega\alpha^2)/(12\upsilon) \quad (4)$$

(where r is the cone radius, ω is the rotational velocity of the cone, α is the cone angle, and ν is the kinematic viscosity of the fluid of interest), is sufficient to characterize laminar and turbulent flow regimes [56]. A numerical solution of the problem may be necessary to examine the detailed and localized nonlinear flow effects at higher pathological or highly variable shear stresses. Under low steady shear stress and with a small cone angle (0.5–1°), the flow is laminar in the rotational direction and inertial effects may be ignored, making the analytical solution approach feasible under such conditions. Another issue with the study of cultured cells is the development of large shear-stress gradients due to undulations at the monolayer surface, which may lead to eddy formation and regions of disturbed flow. Such effects have shown to be reduced on subsequent cell alignment in the direction of flow [57,58]. Thus, in studies involving concurrent shear exposure to cultured and suspended cells under laminar flow conditions, the cultured cells must first be aligned to reduce local secondary flow artifacts. Such secondary flow effects and development of the CPV as a universal device to study both laminar and turbulent flows have been discussed in detail in the following sections.

Modified Reynolds number & CPV

Cox observed secondary flow in the CPV by a dye visualization technique [59]. Sdougos and colleagues later theoretically and experimentally investigated of development of secondary flow in the CPV and showed that a single parameter which is the ratio of centrifugal and viscous flows was sufficient to define limits for laminar and turbulent flow in the CPV [60]. This parameter, $\tilde{\mathrm{Re}}$, defined as the modified Reynolds number (Equation 4), was analogous to earlier independent investigations by Fewell and Hellums [61]. In the limit of $\tilde{\mathrm{Re}} \to 0$, viscous force dominates and primary flow results. In the limit of high $\tilde{\mathrm{Re}}$, the fluid close to the cone experiences outward radial centrifugal force and the fluid close to the plate experiences an inward (opposite) force leading to re-circulation. Well-developed streamlines were observed at $\tilde{\mathrm{Re}}$ less than 0.5, and at a critical $\tilde{\mathrm{Re}}$ greater than 4, turbulent flow was observed. Turbulence was found to originate at the edge of the plate and propagated inward. At high Re, the fluid near the cone experienced higher shear stress and conversely near the plate a lower shear stress, relative to primary flow values. The CPV can thus be used to study development of laminar or turbulent flow for the same shear stress by optimization of $\tilde{\mathrm{Re}}$.

CPV as a turbulent flow device

The turbulent and laminar flow regimes for the CPV was characterized by the modified parameter $\tilde{\mathrm{Re}}$ developed by Sdougos [60], as discussed above. Einav and colleagues extended the application to flow variations in pure turbulent

flow regimes ($\tilde{Re} > 4$) and showed that with increasing rotational velocity of the cone (or increasing $\tilde{Re}$), a three-layer flow structure with distinct boundaries develops [56]. This is characterized by the large azimuthal velocity gradients at the surface and an approximately steady core flow with small linear gradient. The radial velocity profile showed two regions as discussed before, inward flow at the plate and outward flow at the cone surface. The normalized velocity fluctuations in the gap (fluid between the cone and plate) for turbulent flow ($\tilde{Re} > 8$) collapsed into a single curve, analogous to recent findings of similar volume averaged bulk velocity for primary and secondary flows [55]. More importantly, the fluid shear stress at the plate was found to be consistent with experimental results from Sdougos [60] over a wide range of $\tilde{Re}$ values. The CPV can therefore be used to study both laminar and turbulent flows, with the core region between the cone and plate exhibiting homogenous turbulence. A single toroidal vortex was observed by the authors within the secondary flow turbulent region, similar to recent findings by Neelamegham and colleagues [54]. Einav and Grad further experimentally determined the velocity distribution of the fluid (radial and circumferential) in the CPV, thereby proposing constitutive equations for the wall and core flow zones [62]. The wall zones are representative of high viscous forces, whereas Reynolds stresses (centrifugal stresses) dominate the core flow regions. They additionally found that the critical modified Reynolds number ($\tilde{Re}$) for onset of turbulence depends on the surface roughness (of the cone and plate) and the frequency of eddies due to the same can be predicted. In summary, the advantages of the CPV as a turbulent flow device are justified by the following:

- A single parameter $\tilde{Re}$ is sufficient to characterize onset, transition and full development of turbulence in the CPV;
- Instabilities associated with transition from primary to turbulent flow and interaction between the two kinds of flow can be investigated;
- Boundaries demarcating primary and secondary flow are well defined and thus a region of interest can be selected in the CPV;
- Turbulent flow in the CPV is characteristically similar to planar Couette flow (three distinct flow regimes dependent on $\tilde{Re}$), with the core region exhibiting a homogenous turbulent structure over a wide range of $\tilde{Re}$;
- The same system may be used to study laminar or primary flow with the same time averaged shear stresses, for comparison.

Recent investigations on flow transitions in the CPV

The CPV was recently numerically characterized and utilized to investigate neutrophil aggregation under shear stress [54,55]. At higher shear rates, a significant deviation in uniformity of shear stress was observed and caused a multidirectional flow pattern in the CPV and resulted in significantly high hydrodynamic forces on cultured cells and cell suspensions. Under low shear stress conditions and low cone angle, unidirectional flow (often referred to as primary flow) conditions were shown to exist in the CPV. Under such conditions, the rotational velocity component (only nonzero component of the velocity tensor in case of primary flow) can be approximated as ω/α, and is independent of position in the CPV. However at higher shear stresses significant centrifugal forces give rise to disturbed or mixed flow conditions (due to fluid flow radially away from the cone surface), which can be characterized by the Reynolds number and the cone angle. Such nonlinear flow effects on plate surface stress, collision frequency and the rate of aggregation of cell suspensions, were spatially localized to the outer edge of the CPV and were examined in detail. These spatiotemporal variations in local forces may result in incorrect conclusions in biophysical experiments with respect to cellular aggregation and activation (e.g., platelets and neutrophils) and mechanotransduction (ECs). Shankaran and Neelamegham solved the Navier–Stokes and vorticity transport equations to illustrate such local variations in the CPV over a range of shear rates (0–8000 s^{-1}) and cone angles (0.5–2°). Major approximations of the study, however, were the use of a Newtonian fluid model and the absence of fluid interial forces, which may warrant further elucidation when applied to lower shear stresses over whole blood in the CPV. However, such analyses are particularly useful to analyze homotypic and heterotypic cell aggregation by modulation of kinetic on-rates, interaction forces (compressive and tensile), interaction times and collision frequency.

Rotational flow observation & inertial effects in CPV

In a recent study, an optically transparent CPV system, with multiple rheological units and medium-exchange ports, was designed to investigate the effects of laminar or turbulent fluid shear stress on cultured vascular ECs [63]. Development of laminar and turbulent flow patterns was observed by dissolution of a dye on the plate of the CPV. The authors used the modified Reynolds number introduced by Sdougos *et al.* [60] to estimate the upper limit of cone rotational speed for laminar and turbulent flow. More importantly, the authors estimated the characteristic growth time of the shear stress from the cone surface to the plate extrapolated from the Rayleigh solution for fluid between a stationary and a suddenly moving plate. The time scale of these inertial effects is directly proportional to the cone angle, being 0.06 s for a cone angle of 2°. Thus, inertial effects due to rapidly changing shear stress in a dynamic system may be minimized by reducing the cone angle. A numerical investigation of such inertial effects (time-lag until steady state ~0.001 s) and distribution of shear stress in unsteady (oscillating and pulsating) flow in the CPV was recently investigated [64]. The analysis addressed the limitations of analytical solutions for CPV proposed earlier (i.e., infinite radius of the CPV) and suggested numerical calculation to delineate nonuniform shear-stress distribution at high cone rotations ($\omega > 100$ rpm).

Such analyses would be complementary to the analytical solutions proposed earlier by Einav and Sdougos. The minimization of inertial effects in the CPV is absolutely essential to replicate dynamically changing shear stresses encountered in cardiovascular devices.

Hemodynamic shear device

This device was developed in the authors' laboratory, combining cone-plate with cylindrical (coaxial) Couette flow viscometry. The dynamic capabilities are introduced via a programmable interface [24,47]. The device has been successfully used to investigate the shear-induced damage and subsequent recovery of human platelets [65]. A schematic of the device is shown in Figure 1. The HSD is designed such that the shear stresses in both the Couette and cone-and-plate regions are equal, according to the equations:

$$\text{(5)}\quad \tau_{\text{Cone-plate}} = \tau_{\text{Couette}} \rightarrow$$

$$\text{(6)}\quad \mu\frac{\omega}{\alpha} = 2\mu\frac{\omega R_0^2 R_i^2}{R_0^2 - R_i^2}\left(\frac{1}{r^2}\right)\Bigg|_{(r = R_i)}$$

$$\Rightarrow \alpha = \frac{1}{2}\left[1 - \left(\frac{R_i}{R_0}\right)^2\right] (\text{small}\alpha,\ (R_i/R_0) \rightarrow 1)$$

where μ is the kinematic viscosity (1 cP for water or 3 cP for whole blood), ω is the dynamically changing angular velocity of the cone (input via the programmable interface), α is the cone angle, and R_0 and R_i are the inner radius of the outer ring and outer radius of the cone, respectively. In the present design, a 2° cone rests 10 µm above the stationary plate (precision controlled height achieved with a micrometer of 20 µm pitch). The Couette annulus surrounding the cone is 740 µm in width. The dynamics of the system can be optimized by choice of the motor and controller. In the present system, rotational dynamics of the cone were introduced via a stepper motor (Parker Hannifin Corporation, CA, USA), which was programmed with the supplied Motion Architect software (Compumotor6000), and transferred to the cone via a microstepping drive. Rapid changes in cone rotation under highly dynamic conditions may lead to significant secondary flow and development of nonuniform shear stress. We utilize the modified Reynolds number proposed before Equation 4 combining the Reynolds and Womersley numbers, which account for the influences of the local acceleration and centripetal force, respectively) to determine the limit of secondary flow effects [54,55,66].

Potential mixing effects due to the blood–air interface at the top of the Couette region may become apparent only at high shear stresses (τ > 4000 dynes/cm^2) [67]. The present HSD system is capable of a peak shear stress of 65 dynes/cm^2 (for whole blood) before any secondary flow effects become apparent (Re > 0.5). Ultra-high molecular weight polyethylene, which is chemically inert to blood as demonstrated in its use for several biomedical applications [68–70], was utilized to manufacture the cone, base-plate and surrounding ring of the HSD as shown in Figure 1.

Application of the HSD to study platelet activation

Platelets get exposed to substantially varying shear stresses *in vivo*, and mechanisms under which they maintain quiescent or unactivated state may strongly depend on their stress loading

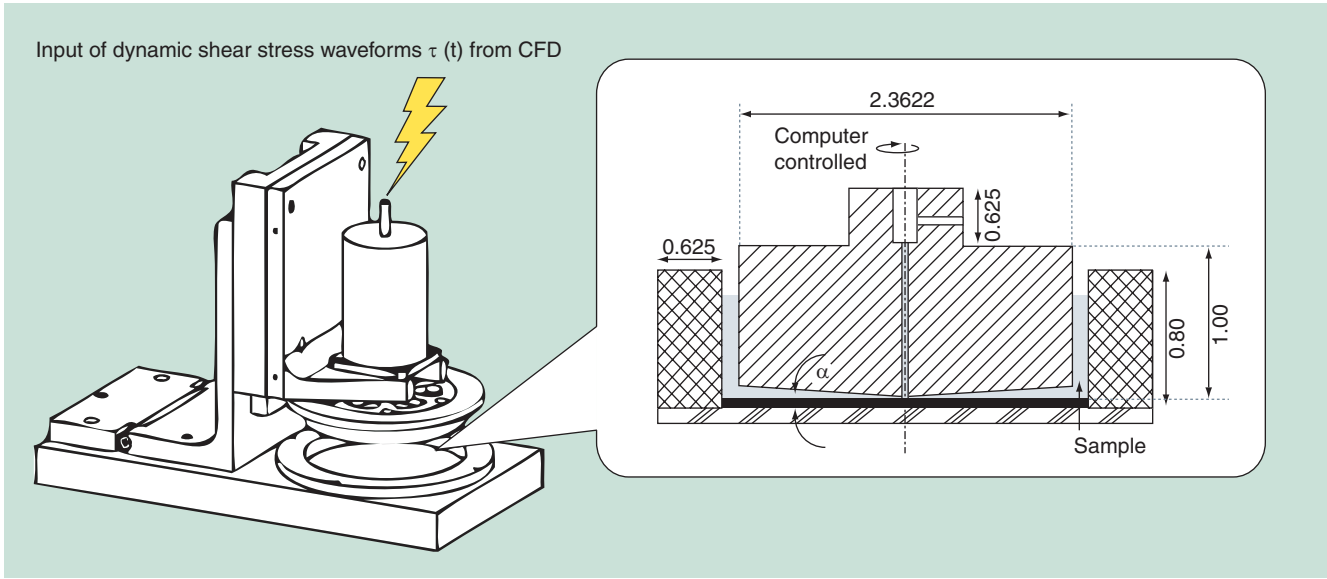

Figure 1. Hemodynamic shear device, consisting of a ring mounted on a stationary plate. Fluid shear stresses are induced by a rotating cone mounted on the shaft of a computer-controlled stepper motor. Platelet samples for platelet activation state assays are drawn from the Couette region, between the rotating cone and mounted ring.

history during circulation. In this study, platelets were exposed to varying shear stress of moderate-to-low magnitude (1.5–20 dynes/cm^2, Figure 2) in the HSD [65] and their instantaneous activation state was measured over time. The platelet membrane damage measured in the HSD and platelet damage accumulation model based on SIPA and genetic algorithm (GA) that predicts this damage were effectively correlated. The study presents an important demonstration of the utility of the HSD to investigate SIPA under dynamically variable shear-stress loading conditions. Specifically, a saw-tooth pattern of shear stress was generated via a programmable interface as discussed previously. The time between the peaks or saw-tooth patterns (T2, Figure 2) was varied from 10 to 60 s to demonstrate time-dependent recovery of platelets from SIPA. Platelets were sampled periodically from the Couette region of the HSD (Figure 1) and their activity was determined using the innovative PAS assay developed in the authors' laboratory [71]. Platelet activity decreased with increasing T2 or 'relaxation time' between the peak shear stress. The experimental results showing platelet damage and recovery under shear stress obtained herein were in excellent agreement with mathematical damage accumulation models proposed by Grigioni *et al.* [72,73], originally developed for RBC hemolysis and adapted for platelets in the study described previously [65].

SIPA during passage through heart valves

Recently, the effect of cumulative stress loading on platelets as they pass through specific areas of MHV were investigated in a 3D numerical model [74]. Blood was modeled as two-phase non-Newtonian fluid, platelets as solid spheres and total particle stress (including intermittent turbulent stresses) was calculated using the Wilcox k-ω turbulence model. Flow conditions were representative of deceleration phase (0.3 s) after peak systole (during which shed vortices and elevated shear stress enhance SIPA). The trajectories of four particles (platelets) and their cumulative stress values as they pass through specific locations in the valve geometry are shown in Figure 3. It can be inferred that geometric irregularities around valve hinges and boundaries lead to elevated cumulative shear stress on the platelets, thus causing activation. The instantaneous shear stress (noncumulative) on these particles is shown in Figure 3. Such stress trajectories may be effectively replicated within the HSD, as discussed in the following section. The HSD – interfaced with the numerical simulations – can be then be used to test design modifications by altering the device geometry in the numerical (virtual) domain, computing the resulting trajectories and their corresponding load histories, and programming the HSD accordingly. Thus, optimization of the thrombogenic performance of the device can be achieved before prototypes are built and tested in costly preclinical trials.

Optimization of HSD to investigate dynamic stresses

Let us consider the stress trajectory with a peak shear stress of 80 dynes/cm^2 (Figure 3). For cone geometry (angle = 0.5°; radius = 0.02 m) and a shear stress of 80 dynes/cm^2, fluid inertial effects (based on first approximation of shear layer growth time) may not be significant (time to steady state ~ 0.003 s). The inertial effects of the system (dynamic response time) may be minimized by choice of a high-peak torque servo motor and controller system, with an external encoder (to obtain position-feedback). The peak modified Reynolds number for this configuration would be 0.013, thereby precluding any secondary flow effects (<10% azimuthal turbulence), as predicted by Einav [56] and Sdougos [60]. The regular Reynolds number can be calculated as 2000 and minimal variation in stream function and shear stress across the fluid (including edge effects) can be predicted [54,55]. The interparticle forces, and adhesion and collision frequency between platelets may be predicted to be close to primary flow [54]. Analysis of the Couette region of the HSD, shows that the Taylor number at peak shear stress would be smaller than the critical value (T = 460; Tc = 1712; T < Tc) for initiation of vortices or significant secondary flow. In the present geometry, the ratio of radii of the inner and outer surface in the annular Couette region is 0.99. Hence the flow in the annular region can be approximated as planar Couette flow. Since onset and dissipation of Taylor vortices and turbulence patterns has been reported over wide ranges, it is difficult to predict the flow behavior for a particular geometry. This can, however, be greatly facilitated by numerical solution coupled with experimental observation at rapid frame rates to isolate localized turbulence occurrences.

Limitations of the HSD

Characterization of flow patterns within HSD for each flow condition may be critical in cases where increased platelet activation cannot be explained on the basis of programmed shear rates and exposure time. Fluid inertia presents a considerable challenge for problems with highly dynamic changes in shear stress that could possibly overwhelm time to reach steady state. Development of an alternative method based on the effect of

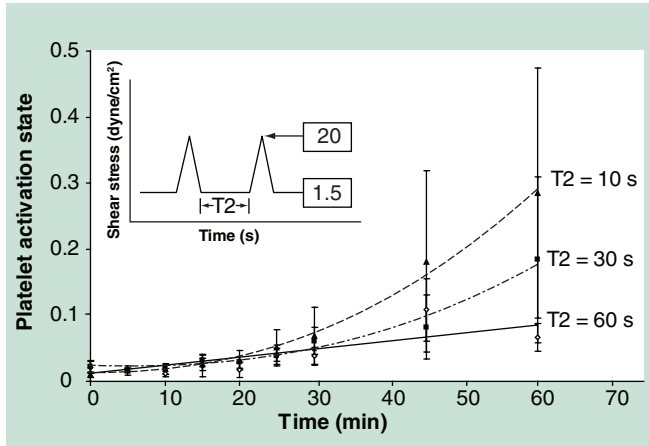

Figure 2. Normalized platelet activation state values for dynamic shear stress waveforms. For T2 = 10 s, mean platelet activation state at 60 min was 0.285 ± 0.189 (SEM), with 0.067 ± 0.021 (SEM) for T2 = 60 s and 0.184 ± 0.125 (SEM) for T2 = 30 s. Adapted from Nobili *et al*. [65].

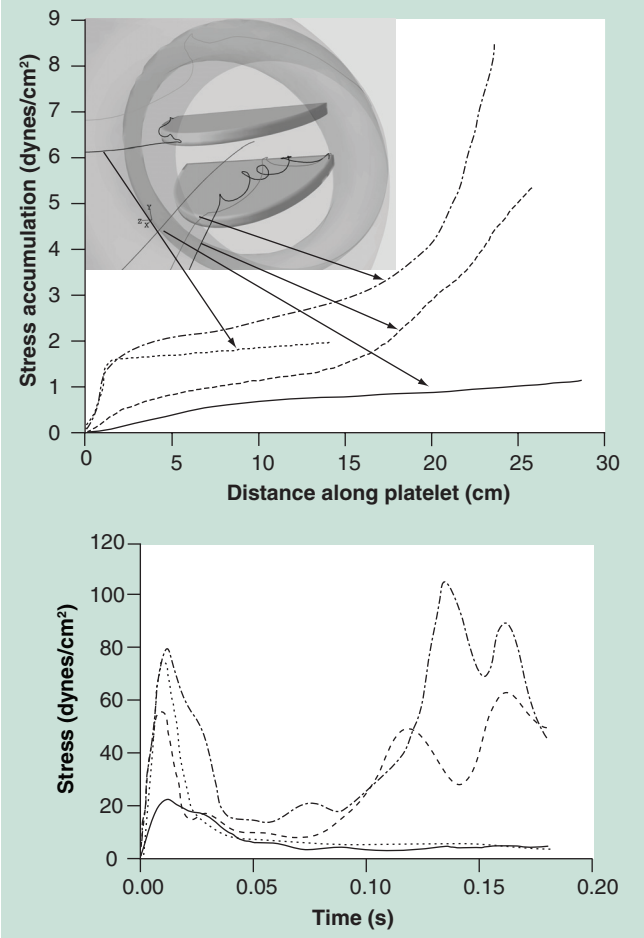

Figure 3. (A) Stress accumulation (platelet level of activation) with the corresponding platelet trajectories. **(B)** Instantaneous stress magnitude on platelets for each trajectory, as shown in **(A).** Adapted from Alemu and Bluestein [74].

cumulative shear stress on platelets may therefore be necessary. Blood is a non-Newtonian fluid and this imposes limitations on direct measurements within the HSD on whole blood at low shear rates, where a bulk viscosity cannot be assumed. In such cases, the effect of shear stress on individual thrombogenic components of blood, such as platelets, can be investigated since a bulk viscosity can then be used, with the same overall shear stress. The air–blood interface at the top of the Couette region in the HSD may introduce significant artifacts at very high ($\tau > 4000$ dynes/cm^2) shear-stress conditions due to secondary flow characteristic of the 'open or free-boundary' Couette flow problem. For better optimization of the present HSD system, the influence of axial flow from the cone region on the annular Couette flow and any fluid mixing effects between the cone and Couette regions need to be numerically characterized for a range of flow conditions. The numerical calculation is also essential to identify the length scales of turbulent eddy in both regions to ascertain their local effects on circulating cells (platelets, RBC or leukocytes). The dynamic range of pathological and dynamic shear stresses may be limited for multicellular environments involving cultured cells which may necessitate the use of larger cone angles (to accommodate larger sample volumes) at which uniformity in applied stresses may be severely compromised. Furthermore, it is nearly impossible to eliminate the occurrence of vortices and regions of variable shear fields within the Couette region of the HSD. However, a numerical approach could be adopted to optimize the annular gap and aspect ratio to minimize such secondary flow effects, over a large dynamic range of shear stresses.

Studies of endothelial cells, RBC, platelets & their interaction

This section summarizes the effects of dynamic shear stress on ECs, RBC and platelets. These effects, distinct from laminar shear stress and implicated in pathophysiology, are key to understanding the development of cardiovascular disease *in vitro* and underscore the need to develop the HSD for this purpose.

Endothelial cells

ECs form the inner lining of blood vessels and are constantly exposed to myriad flow conditions *in vivo* depending on the vasculature. These conditions largely dictate their inflammatory response in the form of altered-adhesion molecule expression [75,76], cytokine secretion [77], leukocyte recruitment and transmigration, and release of vasoactive compounds by mechanotransduction [78]. Although pro- or atherothrombotic flow conditions have been described by several groups, such studies have largely focused on only one cell type and ignored any cell-specific responses in a more complex milieu [49,79,80]. For instance, let us examine the platelet-EC system. Typically low shear-stress conditions with high spatial gradients are believed to be prothrombotic due to decreased release of protective NO derivatives by ECs, increased expression of proinflammatory genes, and increased vascular permeability under those conditions [81–84]. However, such conditions may not cause sufficient shear-induced platelet activation and subsequent aggregation. Conversely, arterial flow conditions favoring significant platelet activation may be atheroprotective from an EC standpoint due to more substantial release of protective vasoactive mediators. Besides the absolute magnitude of shear stress, the complex topography of such stimuli may be critical in examining cell-specific responses. For instance, ECs may be more protective under pulsed shear conditions compared to constant shear stresses, when exposed to the same overall shear stress [48,78,85]. As a corollary, platelets may be prone to higher activation levels when exposed to peak stress waveforms (for instance, when passing through a stenosed region or a heart valve). To date, *in vitro* studies have mostly investigated simple (laminar, pulsatile or oscillating shear stress) alterations in fluid shear stress and their downstream effects.

ECs align parallel to direction of flow under laminar unidirectional shear stress, guided by the structural dynamics of focal adhesions, extracellular matrix (ECM) proteins and

cytoskeletal rearrangements [86]. This flow dependent alignment is strongly influenced by the endothelial glycocalyx, in the absence of which no alignment but increased proliferation occurs [87]. Additionally, the rearrangement of the glycocalyx above the cell–cell contacts after prolonged shear stress exposure is implicated in reducing the shear stress gradients at the surface of the monolayer [87]. Such structural changes in the glycocalyx due to degradation of matrix proteins in atheroprone conditions may also increase the local shear rate at the surface of the cell (EC membrane) [88]. In terms of EC atheroprotective function, disruption of the glycocalyx (heparan sulfate, chondroitin sulfate, hyaluronic acid and oligosaccharides) reduces NO release from the EC [89]. The redistribution of EC surface stresses and subcellular stresses [57,58] and their altered vascular protective function are of key importance when investigating their function under dynamic shear stress *in vitro*.

ECs are constantly subject to normal (blood flow) and circumferential (stretch) stress that are coregulatory in their response to vascular function. Gene expression studies that investigate response of ECs to oscillating or reversed flow at high frequencies show a pronounced increased in proinflammatory profiles (e.g., IL-8 and vascular cell adhesion molecule [VCAM]-1) relative to steady shear stress [85]. Curved regions of the arterial segment, that exhibit disturbed or multidirectional flow, may therefore develop proatherogenic phenotype due to unbalance of stresses leading to disturbed hemostasis [78]. Over the past 20 years, Chien and colleagues have investigated, in detail, the altered gene expression in ECs subject to physiological and pathological shear stress and cyclic stretch [78]. Circumferential stretch in addition to shear stress increases cytoskeletal stress fiber size and orientation synergistically [90], supporting the suppression of proinflammatory gene expression, and increase in anti-inflammatory Jun N terminal Kinase (JNK), Growth arrest and DNA damage inducible gene (*GADD45*), and Kruppel-like factor (KLF2) activity [78]. It should be noted that the timescale of altered vascular function under pathological conditions could be significantly different from other cells under similar conditions. For instance, within the context of developing an *in vitro* system to investigate platelet activation in the presence of ECs under dynamic shear conditions, altered vascular function may first be established by preconditioning the ECs to pathological shear stress (followed by a genetic screening to confirm prothrombotic state) prior to being exposed to platelets.

Red blood cells

RBC constitute 42–46% of the total blood volume. These deformable biconcave disks occupy the center of the blood vessels, leaving approximately 3–6 μm of a plasma-rich layer near the endothelium [91]. Dense RBC envelopes have been shown to significantly enhance leukocyte rolling and adhesion on the endothelium and, subsequently, promote inflammation [92,93]. Under low shear stresses ($\tau < 1$ dyne/cm^2) that favor rouleaux formation, RBC have been shown to significantly adhere to activated platelets, a mechanism proposed for deep-vein thrombosis (DVT) [94]. This evidence suggests that thrombogenesis may be significantly promoted in multicellular environments. An important mechanism for RBC to facilitate platelet adhesion and activation includes the release of ADP from the RBC [95], and this potentiates the thrombogenicity of platelets in multicellular environments [96]. In earlier studies, the chemical and physical effects of RBC on platelets was investigated by Alkhamis and colleagues and they showed that only 2% of the total ADP in the RBC was sufficient to cause platelet activation and aggregation and was nearly 60% of the total ADP released during SIPA [97,98].

Besides influencing thrombogenicity under altered flow conditions, RBC also undergo hemolysis in response to elevated pathological shear stress, often leading to TE and cardioembolic stroke [99]. It has been shown in *in vitro* studies with the Couette viscometer system that RBC hemolyse under shear stress in excess of 1500–4000 dynes/cm^2 [67,100] and the damage is further increased by irregular or dynamic shear patterns [101]. The unique mechanical properties of the RBC wall (spectrin network remodeling [102] and association with the phospholipid bilayer) delineate its ability to rapidly deform (fluidize) and recover its biconcave shape under varying shear stresses [103]. Predominantly high shear stresses over long exposure times are required for RBC hemolysis and such continuum approaches to estimate damage (extreme plasticity) can be integrated with microscale spectrin dynamics models, as a corollary to *in vitro* experiments.

The aggregation of RBC and their effect on the apparent blood viscosity is strongly influenced by the shear rate and has been successfully investigated in optically transparent cone-plate viscometers [104]. Disruption of this normal blood-flow 'structuring' by the RBC leads to local hemorheological disturbances such as local aggregation (leading to increased leukocyte-EC adhesion) in the microvasculature [105]. An optically transparent HSD can therefore be utilized to predict the altered instantaneous dynamic response of RBC (e.g., membrane viscoelasticity and shear modulus) under pathological conditions (e.g., dynamic shear stress waveforms extracted from numerical studies for flow past PHV) as compared to normal physiological flow. Although hemolysis occurs only at very high shear stress and long exposure times ($t > 100$ ms) as mentioned before, observation of RBC-platelet interactions on exposure to intermittent bursts of shear stress such as during passage through the hinge region of PHV, followed by determination of thrombogenic potential, may be substantially useful in optimizing design of such PHV.

Platelets

Platelets (1.5–4-μm disks) are key hemostatic elements involved in plug or clot formation by aggregation, which typically involves platelet surface receptors (glycoprotein 1b and integrin αIIb3), fibrinogen and release of agonists (ADP, thrombin and thromboxane) by activated platelets [106]. In earlier studies on SIPA in the Couette viscometer, Goldsmith and colleagues showed that thrombus formation was significantly enhanced in oscillatory flow whereby platelets have increased collision frequency [107]. The influence of RBC on platelet activation was

later introduced by Sutera *et al.* [47], whereby SIPA and platelet aggregation was confirmed to be significantly greater under pulsatile or dynamic conditions relative to constant shear stress. The effect was more pronounced at shear stress higher than 10 dynes/cm^2, which confirmed the existence of threshold for SIPA [67,108]. Platelet activation, aggregation and microparticle release, either alone or with RBC, on exposure to normal or pathological shear stress have since been extensively investigated in cone and plate or Couette viscometers [46,51,52,109–112]. However, these studies did not consider diverse flow dynamics and their effects on SIPA such as stagnation, flow reversal, local turbulence and eddy currents, as might be expected *in vivo* when platelets pass through complex geometries.

Platelet activation under such physiological flow trajectories have been investigated in recirculation devices for flow past PHV [4–6]. Additionally, numerical calculations also show the cumulative effect of shear stress and exposure time (spatio-temporal) on platelet activation under such conditions [9–11]. It has also been shown that SIPA and thrombin generation is strongly influenced by platelet counts and platelet-platelet cooperativity [113]. Such effects may therefore be substantially enhanced due to recirculation within Taylor vortices, where the duration of shear exposure and platelet–platelet collisions may be significantly increased relative to bulk flow. The shear stresses due to such flow effects can be effectively reproduced in Couette viscometers by appropriate choice of geometrical (e.g., radius ratio of the inner rotating and outer stationary cylinders, and aspect ratio, of the Couette viscometer) and experimental (e.g., rotational velocity and acceleration of the inner cylinder, viscosity of the fluid and overall shear stress) parameters [31,37]. Shear stress waveforms from numerical simulations may thus be reproduced *in vitro* with a dynamically controlled viscometer and thrombin generation from shear-stress activated platelets can be measured to determine thrombogenicity associated with PHV or recirculation devices.

Platelets are exposed to continuously varying shear stress *in vivo*. The average transit times of platelets through regions of high cumulative shear stress may be relatively small compared with the overall transit through the vasculature. This may allow the platelets to recover or reverse their activated state and regain their discoid shape. The mechanics and kinetics of recovery of platelets after acute shear-stress exposure have been recently experimentally investigated in the HSD as discussed previously [65]. These results show remarkable agreement with numerical predictions from a cumulative damage accumulation model (i.e., cumulative effect of previous activated state, shear loading history and exposure time) originally proposed to investigate RBC hemolysis [72,73]. More importantly, the study demonstrates the utility of dynamic viscometers in emulating shear-loading histories (and determination of their effects on platelets) typically found in arterial circulation and recirculation devices.

Prominent methods to determine platelet activation include measuring change in expression of cell-surface receptors by flow cytometry, rate of platelet aggregation with agonist (thrombin receptor activators or calcium ionophore) treatment, and rate of thrombin generation as a function of Factor Va release by platelets [71,114,115]. Of these methods, the direct measurement of thrombin generation without feedback has been developed in the authors' laboratory and is a highly reliable method (~0.1% relative error) for determining the rate of platelet activation and hence thrombogenicity of recirculation devices [116]. This method can be utilized to determine SIPA in dynamic viscometers as a corollary to that determined in recirculation devices to accurately identify shear-stress trajectories that cause significant platelet activation. Using the aforementioned approaches, the design of PHV or recirculation devices can therefore be optimized to minimize thrombogenicity.

Expert commentary

The purpose of the HSD, as discussed in this review, is to be able to replicate shear-stress patterns in and around PHV and other cardiovascular prosthetic devices geometries calculated numerically using novel approaches as discussed previously by the author [117]. Once design optimization has been achieved numerically to minimize the predicted cumulative platelet damage in recirculation devices and PHV [74], the dynamic shear stress information can be fed to the HSD and the effect of such localized stress trajectories on platelet activation can be accurately assessed *in vitro*. The basic advantage is the accentuation of specific shear stresses due to minute design alterations of PHV, on damage or activation of cells of interest. Further optimization of this top-down approach would therefore facilitate the least thrombogenic design for the implantable device. Thus, significant cost minimization can be achieved before expensive prototypes are developed and tested in preclinical trials.

The CPV analysis, analytically and experimentally investigated by various groups (e.g., Einav, Neelamegham and Schnittler), has established CPV as a compact flow system to study both laminar and turbulent shear stresses and the interaction between them in distinct regions. With the CPV, both laminar and turbulent stresses can be generated for the same time-averaged shear stress. The characteristics of flow in the CPV can be defined and controlled with two parameters: the modified Reynolds number and the cone angle. Optimization of the geometry thus provides an invaluable solution to investigate a wide range of shear stresses and flow patterns (extracted from *in vivo* measurements or from numerical simulations) in the CPV. At higher speeds of rotation (corresponding to pathological shear stresses), a numerical solution can provide accurate localized stress distribution. The lag-time associated with the CPV is of the order of 0.001 s and is inversely related to the cone angle. Thus, highly dynamic shear-stress trajectories can be investigated for their temporal effects on cells and interactions between them.

The basic advantage of integrating the CPV with Couette flow in our HSD device is to facilitate sampling from the Couette region of the cell sample of interest to investigate real-time

changes in activation state. Since the Couette region has a large aspect ratio (70) and radius ratio close to 1 (0.99), the flow can be approximated as planar Couette and may be further characterized by Taylor number for the fluid of interest. For a narrow gap, the inertial effects can therefore be predicted to be of the same scale as those found for the CPV. Detailed flow patterns in both the CPV and Couette viscometer have been investigated extensively and are beyond the scope of this review. Of pertinent interest is the ability to replicate highly complex shear-stress trajectories without considerable inertial and secondary flow effects, for their localized and integrated effects on cell populations.

Five-year view

Several advances to optimize *in vivo* device thrombogenicity by developing dynamic *in vitro* devices can be made over the next 5 years. With the advancement of technology and availability of highly dynamic motor-controller systems, the HSD can be optimized for high temporal-sensitivity measurements. Rapid advancement in numerical techniques now incorporating fluid structure interaction and effects of localized particle concentrations, will further facilitate more accurate extraction of thrombogenic flow patterns in and around devices and replicate them for *in vitro* experiments. Furthermore, it will facilitate more accurate replication of normal and pathophysiological flow conditions in the vascalture, under which interaction of various blood constituents with the endothelium would be critical for advancing our understanding of the progression of cardiovascular disease. Progress on all these fronts would enable the HSD and similar compact *in vitro* systems to emerge as invaluable tools for device thrombogenicity optimization and development of *in vitro* disease models.

Financial & competing interests disclosure

The authors have no relevant affiliations or financial involvement with any organization or entity with a financial interest in or financial conflict with the subject matter or materials discussed in the manuscript. This includes employment, consultancies, honoraria, stock ownership or options, expert testimony, grants or patents received or pending, or royalties.

No writing assistance was utilized in the production of this manuscript.

Key issues

- Prosthetic blood recirculating cardiovascular devices such as prosthetic heart valves induce the emergence of pathologic-flow patterns, such as shed vortices and turbulence, elevating the stress levels to which blood constituents are exposed to, which may lead to thromboembolism even with the administration of anticoagulation.
- The thrombogenic effects of local shear-stress trajectories in these devices cannot be determined from bulk platelet activation measurements in the device – a compact programmable dynamic *in vitro* system interfaced to numerical simulations can address this.
- Accentuation of the minute and very specific effects of device design modifications (such as local shear-stress trajectories mentioned above) on cell suspensions can be accomplished in a viscometer, which could then be a universal (device independent) thrombogenicity testing tool for any blood recirculation device for its design optimization.
- The cone and plate viscometer (CPV) has been established as a compact flow system for investigating laminar and turbulent flow conditions.
- In CPV systems, the extent of secondary flow and its influence on particle dynamics, cell–cell interaction and distribution shear stress can be determined with by controlling two main parameters: modified Reynolds number and cone angle.
- The annular Couette flow device has been widely used for determining shear-induced hematological damage (platelets and red cells), and can be effectively integrated with the CPV into one device (hemodynamic shear device).
- Complex dynamic flow patterns are capable of conferring very distinct functional effects on vascular endothelial cells, platelets and red blood cells, and can be tested in such compact systems under wide range of pathophysiological flow conditions.
- The thromogenic potential of cardiovascular devices (e.g., prosthetic heart valves) can be optimized in the numerical (virtual) domain and the optimization then tested in the hemodynamic shear device, in order to achieve thrombogenicity optimization for the device before costly prototypes are built and preclinically tested.

References

Papers of special note have been highlighted as:

- • of interest
- •• of considerable interest

1 Bodnar E. The Medtronic Parallel valve and the lessons learned. *J. Heart Valve Dis.* 5(6), 572–573 (1996).

2 Antunes MJ, Colsen PR, Kinsley RH. Intermittent aortic regurgitation following aortic valve replacement with the Hall–Kaster prosthesis. *J. Thorac. Cardiovasc. Surg.* 84(5), 751–754 (1982).

3 Omoto R, Matsumura M, Asano H *et al.* Doppler ultrasound examination of prosthetic function and ventricular blood flow after mitral valve replacement. *Herz* 11(6), 346–350 (1986).

4 Yin W, Krukenkamp IB, Saltman AE *et al.* Thrombogenic performance of a St. Jude bileaflet mechanical heart valve in a sheep model. *ASAIO J.* 52(1), 28–33 (2006).

5 Yin W, Gallocher S, Pinchuk L *et al.* Flow-induced platelet activation in a St. Jude mechanical heart valve, a trileaflet polymeric heart valve, and a St. Jude tissue valve. *Artif. Organs* 29(10), 826–831 (2005).

6 Yin W, Alemu Y, Affeld K, Jesty J, Bluestein D. Flow-induced platelet activation in bileaflet and monoleaflet mechanical heart valves. *Ann. Biomed. Eng.* 32(8), 1058–1066 (2004).

7 Bluestein D, Yin W, Affeld K, Jesty J. Flow-induced platelet activation in mechanical heart valves. *J. Heart Valve Dis.* 13(3), 501–508 (2004).

• **Utility of the innovative platelet activation state (PAS) assay to determine procoagulant properties of platelets by flow through mechanical heart valves.**

8 Dumont K, Vierendeels J, van Nooten G, Verdonck P, Bluestein, D. Comparison of ATS Open Pivot Valve and St Jude Regent Valve using a CFD model based on fluid-structure interaction. *J. Biomech. Eng.* 129(4) (2007).

9 Travis BR, Marzec UM, Ellis JT *et al.* The sensitivity of indicators of thrombosis initiation to a bileaflet prosthesis leakage stimulus. *J. Heart Valve Dis.* 10(2), 228–238 (2001).

10 Simon HA, Dasi LP, Leo HL, Yoganathan AP. Spatio–temporal flow analysis in bileaflet heart valve hinge regions: potential analysis for blood element damage. *Ann. Biomed. Eng.* 35(8), 1333–1346 (2007).

11 Leo HL, Simon HA, Dasi LP, Yoganathan AP. Effect of hinge gap width on the microflow structures in 27-mm bileaflet mechanical heart valves. *J. Heart Valve Dis.* 15(6), 800–808 (2006).

12 Raz S, Einav S, Alemu Y, Bluestein D. DPIV prediction of flow induced platelet activation-comparison to numerical predictions. *Ann. Biomed. Eng.* 35(4), 493–504 (2007).

13 Dintenfass L, Julian DG, Miller GE. Viscosity of blood in normal subjects and in patients suffering from coronary occlusion and arterial thrombosis. An *in vitro* study in the absence of anticoagulants, by means of a rotational cone-in-cone trolley viscometer. *Am. Heart J.* 71(5), 587–600 (1966).

14 Evans A, Weaver JP, Walder DN. A viscometer for the study of blood. *Biorheology* 4(4), 169–174 (1967).

15 Skovborg F, Nielsen AV, Schlichtkrull J. Blood viscosity and vascular flow rate. Blood-viscosity measured in a cone-plate viscometer and the flow rate in an isolated vascular bed. *Scand. J. Clin. Lab. Invest.* 21(1), 83–88 (1968).

16 Larsson H, Odeberg H, Bohlin L. Studies of blood viscosity with a newly constructed rotational viscometer which operates via a desk top computer. *Scand. J. Clin. Lab. Invest.* 43(6), 493–502 (1983).

17 McMillan DE, Utterback NG, Nasrinasrabadi M, Lee MM. An instrument to evaluate the time dependent flow properties of blood at moderate shear rates. *Biorheology* 23(1), 63–74 (1986).

18 Paul R, Apel J, Klaus S *et al.* Shear stress related blood damage in laminar couette flow. *Artif. Organs* 27(6), 517–529 (2003).

19 Cokelet GR, Brown JR, Codd SL, Seymour JD. Magnetic resonance microscopy determined velocity and hematocrit distributions in a Couette viscometer. *Biorheology* 42(5), 385–399 (2005).

20 Heuser G, Opitz R. A Couette viscometer for short time shearing of blood. *Biorheology* 17(1–2), 17–24 (1980).

21 Reinhart WH, Hausler K, Schaller P *et al.* Rheological properties of blood as assessed with a newly designed oscillating viscometer. *Clin. Hemorheol. Microcirc.* 18(1), 59–65 (1998).

22 Voisin P, Guimont C, Stoltz JF. Experimental investigation of the rheological activation of blood platelets. *Biorheology* 22(5), 425–435 (1985).

23 Wang X, Liao FL, Stoltz JF. A new simple cone-plate viscometer for hemorheology. *Clin. Hemorheol. Microcirc.* 19(1), 25–31 (1998).

24 Blackman BR, Barbee KA, Thibault LE. *In vitro* cell shearing device to investigate the dynamic response of cells in a controlled hydrodynamic environment. *Ann. Biomed. Eng.* 28(4), 363–372 (2000).

•• **Introduction of the dynamic computer-controlled high-precision cone and plate viscometer (CPV) shear device – precursor to the hemodynamic shear device.**

25 Yeh C, Calvez AC, Eckstein EC. An estimated shape function for drift in a platelet-transport model. *Biophys. J.* 67(3), 1252–1259 (1994).

26 Yeh C, Eckstein EC. Transient lateral transport of platelet-sized particles in flowing blood suspensions. *Biophys. J.* 66(5), 1706–1716 (1994).

27 Hung TC, Hochmuth RM, Joist JH, Sutera SP. Shear-induced aggregation and lysis of platelets. *Trans. Am. Soc. Artif. Intern. Organs* 22, 285–291 (1976).

28 Klaus S, Korfer S, Mottaghy K, Reul H, Glasmacher B. *In vitro* blood damage by high shear flow: human versus porcine blood. *Int. J. Artif. Organs* 25(4), 306–312 (2002).

29 Taylor GI. Stability of a viscous liquid contained between two rotating cylinders. *Phil. Trans. Roy. Soc. (London)* A223, 289–343 (1923).

30 Chandrasekhar S. The hydrodynamic stability of viscid flow between coaxial cylinders. *Proc. Natl Acad. Sci. USA* 46(1), 141–143 (1960).

31 Czarny O, Lueptow RM. Time scales for transition in Taylor–Couette flow. *Phys. Fluids* 19(5) 054103 (2007).

32 Dutcher CS, Muller SJ. Explicit analytic formulas for Newtonian Taylor–Couette primary instabilities. *Phys. Rev. E. Stat. Nonlin. Soft Matter Phys.* 75(4 Pt 2), 047301 (2007).

33 Korfer S, Klaus S, Mottaghy K. Application of Taylor vortices in hemocompatibility investigations. *Int. J. Artif. Organs* 26(4), 331–338 (2003).

34 Kim MC, Chung TJ, Choi CK. The onset of Taylor-like vortices in the flow induced by an impulsively started rotating cylinder. *Theor. Comp. Fluid Dyn.* 18(2–4), 105–114 (2004).

35 Chandrasekhar S. *Hydrodynamic and Hydromagnetic Stability.* (Eds). Oxford University Press, NY, USA (1961).

36 Kim MC, Choi CK. The onset of instability in the flow induced by an impulsively started rotating cylinder. *Chem. Eng. Sci.* 60(3), 599–608 (2005).

37 Diprima RC, Eagles PM, Ng BS. The effect of radius ratio on the stability of Couette-flow and Taylor vortex flow. *Phys. Fluids* 27(10), 2403–2411 (1984).

38 Cole JA. Taylor-Vortex Instability and Annulus-Length Effects. *J. Fluid Mech.* 75, 1–15 (1976).

39 Lim TT, Chew YT, Xiao Q. A new flow regime in a Taylor-Couette flow. *Phys. Fluids* 10(12), 3233–3235 (1998).

40 Batten WM, Bressloff NW, Turnock SR. Numerical simulations of the evolution of Taylor cells from a growing boundary layer on the inner cylinder of a high radius ratio Taylor-Couette system. *Phys. Rev. E. Stat. Nonlin. Soft Matter Phys.* 66(6 Pt 2), 066302 (2002).

41 Wu J, Antaki JF, Snyder TA *et al.* Design optimization of blood shearing instrument by computational fluid dynamics. *Artif. Organs* 29(6), 482–489 (2005).

42 Mooney M, Ewart RH. The coincylindrical viscometer. *Physics* 5, 350–354 (1934).

43 Wells RE Jr, Denton R, Merrill EW. Measurement of viscosity of biologic fluids by cone plate viscometer. *J. Lab. Clin. Med.* 57, 646–656 (1961).

44 Williams AR, Escoffery CT, Gorst DW. The fragility of normal and abnormal erythrocytes in a controlled hydrodynamic shear field. *Br. J. Haematol.* 37(3), 379–389 (1977).

45 Schwartz JA, Keagy BA, Johnson G Jr. Determination of whole blood apparent viscosity: experience with a new hemorheologic technique. *J. Surg. Res.* 45(2), 238–247 (1988).

46 Giorgio TD, Hellums JD. A cone and plate viscometer for the continuous measurement of blood platelet activation. *Biorheology* 25(4), 605–624 (1988).

47 Sutera SP, Nowak MD, Joist JH, Zeffren DJ, Bauman JE. A programmable, computer-controlled cone-plate viscometer for the application of pulsatile shear stress to platelet suspensions. *Biorheology* 25(3), 449–459 (1988).

• **First introduction of the programmable CPV device and application.**

48 Blackman BR, Garcia-Cardena G, Gimbrone MA Jr. A new *in vitro* model to evaluate differential responses of endothelial cells to simulated arterial shear stress waveforms. *J. Biomech. Eng.* 124(4), 397–407 (2002).

• **Application of the computer-controlled CPV to investigate effect of dynamic waveforms on cultured cells.**

49 Hastings NE, Simmers MB, McDonald OG, Wamhoff BR, Blackman BR. Atherosclerosis-prone hemodynamics differentially regulates endothelial and smooth muscle cell phenotypes and promotes pro-inflammatory priming. *Am. J. Physiol. Cell Physiol.* 293(6),C1824–C1833 (2007).

50 Simmers MB, Pryor AW, Blackman BR. Arterial shear stress regulates endothelial cell-directed migration, polarity, and morphology in confluent monolayers. *Am. J. Physiol. Heart Circ. Physiol.* 293(3), H1937–H1946 (2007).

51 Ohshima N, Onohara M, Sato M. Dynamics of platelet adhesion to artificial materials and cultured endothelial cells under shear flow. *ASAIO Trans.* 35(3), 379–381 (1989).

52 Rhodes NP, Shortland AP, Rattray A, Williams DF. Platelet reactions to modified surfaces under dynamic conditions. *J. Mater. Sci. Mater. Med.* 9(12), 767–772 (1998).

53 Peerschke EI, Silver RT, Weksler B *et al.* *Ex vivo* evaluation of erythrocytosis-enhanced platelet thrombus formation using the cone and plate(let) analyzer: effect of platelet antagonists. *Br. J. Haematol.* 127(2), 195–203 (2004).

54 Shankaran H, Neelamegham S. Nonlinear flow affects hydrodynamic forces and neutrophil adhesion rates in cone-plate viscometers. *Biophys. J.* 80(6), 2631–2648 (2001).

•• **Comprehensive numerical and experimental study on secondary flow effects in the CPV and neutrophil aggregation.**

55 Shankaran H, Neelamegham S. Effect of secondary flow on biological experiments in the cone-plate viscometer: methods for estimating collision frequency, wall shear stress and inter-particle interactions in non-linear flow. *Biorheology* 38(4), 275–304 (2001).

• **Multiparameter numerical study on secondary flow in CPV; shows that Reynolds number and cone angle govern secondary flow.**

56 Einav S, Dewey CF, Hartenbaum H. Cone-and-plate apparatus – a compact system for studying well-characterized turbulent-flow fields. *Exp. Fluids* 16(3–4), 196–202 (1994).

•• **Analytical characterization of turbulent zones within the CPV and the critical Reynolds number for turbulent flow.**

57 Barbee KA, Mundel T, Lal R, Davies PF. Subcellular distribution of shear stress at the surface of flow-aligned and nonaligned endothelial monolayers. *Am. J. Physiol.* 268(4 Pt 2), H1765–H1772 (1995).

58 Barbee KA. Role of subcellular shear-stress distributions in endothelial cell mechanotransduction. *Ann. Biomed. Eng.* 30(4), 472–482 (2002).

59 Cox DB. Radial flow in cone-plate viscometer. *Nature* 193(4816), 670 (1962).

60 Sdougos HP, Bussolari SR, Dewey CF. Secondary Flow and Turbulence in a Cone-and-Plate Device. *J. Fluid Mech.* 138, 379–404 (1984).

•• **First introduction of the modified Reynolds number to characterize laminar and turbulent flow in the CPV.**

61 Fewell ME, Hellums JD. The secondary flow of Newtonian fluids in cone-and-plate viscometers. *Trans. Soc. Rheol.* 21, 535–565 (1977).

62 Grad Y, Einav S. Spectral and instantaneous flow field characteristics of the laminar to turbulent transition in a cone and plate apparatus. *Exp. Fluids* 28(4), 336–343 (2000).

• **Observation of turbulent zones in the CPV and implications of surface roughness on the critical Reynolds number for turbulent flow.**

63 Schnittler HJ, Franke RP, Akbay U, Mrowietz C, Drenckhahn D. Improved *in vitro* rheological system for studying the effect of fluid shear stress on cultured cells. *Am. J. Physiol.* 265(1 Pt 1), C289–C298 (1993).

64 Buschmann MH, Dieterich P, Adams NA, Schnittler HJ. Analysis of flow in a cone-and-plate apparatus with respect to spatial and temporal effects on endothelial cells. *Biotechnol. Bioeng.* 89(5), 493–502 (2005).

•• **Determination of shear stress distribution on cultured cells and estimation of the time taken to achieve steady state for unsteady flow in CPV.**

65 Nobili M, Sheriff JF, Morbiducci U, Redaelli A, Bluestein D. Platelet activation due to hemodynamic shear stresses: damage accumulation model and comparison to *in vitro* measurements. *ASAIO J.* (In Press) (2008).

•• **First application of the hemodynamic shear device to study shear induced platelet activation.**

66 Chung CA, Tzou MR, Ho RW. Oscillatory flow in a cone-and-plate bioreactor. *J. Biomech. Eng.* 127(4), 601–610 (2005).

67 Leverett LB, Hellums JD, Alfrey CP, Lynch EC. Red blood cell damage by shear stress. *Biophys. J.* 12(3), 257–273 (1972).

68 Wolf C, Lederer K, Pfragner R *et al.* Biocompatibility of ultra-high molecular weight polyethylene (UHMW-PE) stabilized with α-tocopherol used for joint endoprostheses assessed *in vitro*. *J. Mater. Sci. Mater. Med.* 18(6), 1247–1252 (2007).

69 Wolf C, Lederer K, Bergmeister H, Losert U, Bock P. Animal experiments with ultra-high molecular weight polyethylene (UHMW-PE) stabilised with α-tocopherol used for articulating surfaces in joint endoprostheses. *J. Mater. Sci. Mater. Med.* 17(12), 1341–1347 (2006).

70 Klapperich C, Pruitt L, Komvopoulos K. Chemical and biological characteristics of low-temperature plasma treated ultra-high molecular weight polyethylene for biomedical applications. *J. Mater. Sci. Mater. Med.* 12(6), 549–556 (2001).

71 Jesty J, Bluestein D. Acetylated prothrombin as a substrate in the measurement of the procoagulant activity of platelets: elimination of the feedback activation of platelets by thrombin. *Anal. Biochem.* 272(1), 64–70 (1999).

• **The innovative PAS assay for real-time measurement of platelet activation via thrombin generation without feedback.**

72 Grigioni M, Daniele C, Morbiducci U *et al.* The power-law mathematical model for blood damage prediction: analytical developments and physical inconsistencies. *Artif. Organs* 28(5), 467–475 (2004).

73 Grigioni M, Morbiducci U, D'Avenio G, Benedetto GD, Gaudio CD. A novel formulation for blood trauma prediction by a modified power-law mathematical model. *Biomech. Model Mechanobiol.* 4(4), 249–260 (2005).

74 Alemu Y, Bluestein D. Flow-induced platelet activation and damage accumulation in a mechanical heart valve: numerical studies. *Artif. Organs* 31(9), 677–688 (2007).

- **Shear induced cumulative platelet activation as it passes through geometrical constrictions in the prosthetic heart valves (PHV).**

75 McKinney VZ, Rinker KD, Truskey GA. Normal and shear stresses influence the spatial distribution of intracellular adhesion molecule-1 expression in human umbilical vein endothelial cells exposed to sudden expansion flow. *J. Biomech.* 39(5), 806–817 (2006).

76 Methe H, Balcells M, Alegret Mdel C *et al.* Vascular bed origin dictates flow pattern regulation of endothelial adhesion molecule expression. *Am. J. Physiol. Heart Circ. Physiol.* 292(5), H2167–H2175 (2007).

77 Matsumoto Y, Kawai Y, Watanabe K *et al.* Fluid shear stress attenuates tumor necrosis factor-alpha-induced tissue factor expression in cultured human endothelial cells. *Blood* 91(11), 4164–4172 (1998).

78 Chien S. Mechanotransduction and endothelial cell homeostasis: the wisdom of the cell. *Am. J. Physiol. Heart Circ. Physiol.* 292(3), H1209–1224 (2007).

- **Comprehensive review of the effect of shear stress and cyclic strain on endothelial cells (ECs).**

79 Grabowski EF, Lam FP. Endothelial cell function, including tissue factor expression, under flow conditions. *Thromb. Haemost.* 74(1), 123–128 (1995).

80 Grabowski EF. Thrombolysis, flow, and vessel wall interactions. *J. Vasc. Interv. Radiol.* 6(6 Pt 2 Su), 25S-29S (1995).

81 Ku DN, Giddens DP, Zarins CK, Glagov S. Pulsatile flow and atherosclerosis in the human carotid bifurcation. Positive correlation between plaque location and low oscillating shear stress. *Arteriosclerosis* 5(3), 293–302 (1985).

82 Kaazempur-Mofrad MR, Isasi AG, Younis HF *et al.* Characterization of the atherosclerotic carotid bifurcation using MRI, finite element modeling, and histology. *Ann. Biomed. Eng.* 32(7), 932–946 (2004).

83 Chen BP, Li YS, Zhao Y *et al.* DNA microarray analysis of gene expression in endothelial cells in response to 24-h shear stress. *Physiol. Genomics* 7(1), 55–63 (2001).

84 Chien S. Molecular and mechanical bases of focal lipid accumulation in arterial wall. *Prog. Biophys. Mol. Biol.* 83(2), 131–151 (2003).

85 Himburg HA, Dowd SE, Friedman MH. Frequency-dependent response of the vascular endothelium to pulsatile shear stress. *Am. J. Physiol. Heart Circ. Physiol.* 293(1), H645–653 (2007).

86 Mott RE, Helmke BP. Mapping the dynamics of shear stress induced structural changes in endothelial cells. *Am. J. Physiol. Cell Physiol.* 293(5), C1616–C1626 (2007).

87 Yao Y, Rabodzey A, Forbes Dewey C Jr. Glycocalyx modulates the motility and proliferative response of vascular endothelium to fluid shear stress. *Am. J. Physiol. Heart Circ. Physiol.* 293(2), H1023–H1030 (2007).

88 Wang W. Change in properties of the glycocalyx affects the shear rate and stress distribution on endothelial cells. *J. Biomech. Eng.* 129(3), 324–329 (2007).

89 Pahakis MY, Kosky JR, Dull RO, Tarbell JM. The role of endothelial glycocalyx components in mechanotransduction of fluid shear stress. *Biochem. Biophys. Res. Commun.* 355(1), 228–233 (2007).

90 Zhao S, Suciu A, Ziegler T *et al.* Synergistic effects of fluid shear stress and cyclic circumferential stretch on vascular endothelial cell morphology and cytoskeleton. *Arterioscler. Thromb. Vasc. Biol.* 15(10), 1781–1786 (1995).

91 Skalak R, Chien S. *Handbook of Bioengineering.* (Eds). McGraw-Hill, New York, NY, USA (1987).

92 Melder RJ, Yuan J, Munn LL, Jain RK. Erythrocytes enhance lymphocyte rolling and arrest *in vivo*. *Microvasc.Res.*, 59(2), 316–322 (2000).

93 Munn LL, Melder RJ, Jain RK. Role of erythrocytes in leukocyte-endothelial interactions: mathematical model and experimental validation. *Biophys. J.* 71(1), 466–478 (1996).

94 Goel MS, Diamond SL. Adhesion of normal erythrocytes at depressed venous shear rates to activated neutrophils, activated platelets, and fibrin polymerized from plasma. *Blood* 100(10), 3797–3803 (2002).

95 Joist JH, Bauman JE, Sutera SP. Platelet adhesion and aggregation in pulsatile shear flow: effects of red blood cells. *Thromb. Res.* 92(6 Suppl. 2), S47–S52 (1998).

96 Turitto VT, Weiss HJ. Red blood cells: their dual role in thrombus formation. *Science* 207(4430), 541–543 (1980).

97 Alkhamis TM, Beissinger RL, Chediak JR. Red blood cell effect on platelet adhesion and aggregation in low-stress shear flow. Myth or fact? *ASAIO Trans.* 34(3), 868–873 (1988).

98 Alkhamis TM, Beissinger RL, Chediak JR. Artificial surface effect on red blood cells and platelets in laminar shear flow. *Blood* 75(7), 1568–1575 (1990).

99 Wurzinger LJ, Blasberg P, Schmid-Schonbein H. Towards a concept of thrombosis in accelerated flow: rheology, fluid dynamics, and biochemistry. *Biorheology* 22(5), 437–450 (1985).

100 Sallam AM, Hwang NH. Human red blood cell hemolysis in a turbulent shear flow: contribution of Reynolds shear stresses. *Biorheology* 21(6), 783–797 (1984).

101 Zhao R, Antaki JF, Naik T *et al.* Microscopic investigation of erythrocyte deformation dynamics. *Biorheology* 43(6), 747–765 (2006).

102 An X, Lecomte MC, Chasis JA, Mohandas N, Gratzer W. Shear-response of the spectrin dimer-tetramer equilibrium in the red blood cell membrane. *J. Biol. Chem.* 277(35), 31796–31800 (2002).

103 Li J, Lykotrafitis G, Dao M, Suresh S. Cytoskeletal dynamics of human erythrocyte. *Proc. Natl Acad. Sci. USA* 104(12), 4937–4942 (2007).

104 Schmid-Schonbein H, Gaehtgens P, Hirsch H. On the shear rate dependence of red cell aggregation *in vitro*. *J. Clin. Invest.* 47(6), 1447–1454 (1968).

105 McHedlishvili G. Disturbed blood flow structuring as critical factor of hemorheological disorders in microcirculation. *Clin. Hemorheol. Microcirc.* 19(4), 315–325 (1998).

106 Jackson SP. The growing complexity of platelet aggregation. *Blood* 109(12), 5087–5095 (2007).

107 Goldsmith HL, Yu SS, Marlow J. Fluid mechanical stress and the platelet. *Thromb. Diath. Haemorrh.* 34(1), 32–41 (1975).

108 Brown CH 3rd, Leverett LB, Lewis CW, Alfrey C Jr, Hellums JD. Morphological, biochemical, and functional changes in human platelets subjected to shear stress. *J. Lab. Clin. Med.* 86(3), 462–471 (1975).

109 Feng S, Lu X, Resendiz JC, Kroll MH. Pathological shear stress directly regulates platelet αIIbβ3 signaling. *Am. J. Physiol. Cell Physiol.* 291(6), C1346–C1354 (2006).

110 Konstantopoulos K, Wu KK, Udden MM *et al.* Flow cytometric studies of platelet responses to shear stress in whole blood. *Biorheology* 32(1), 73–93 (1995).

111 Leytin V, Allen DJ, Mykhaylov S *et al.* Pathologic high shear stress induces apoptosis events in human platelets. *Biochem. Biophys. Res. Commun.* 320(2), 303–310 (2004).

112 Pontiggia L, Steiner B, Ulrichts H *et al.* Platelet microparticle formation and thrombin generation under high shear are effectively suppressed by a monoclonal antibody against GPIba. *Thromb. Haemost.* 96(6), 774–780 (2006).

113 Schulz-Heik K, Ramachandran J, Bluestein D, Jesty J. The extent of platelet activation under shear depends on platelet count: differential expression of anionic phospholipid and Factor Va. *Pathophysiol. Haemost. Thromb.* 34(6), 255–262 (2005).

114 Shah U, Ma AD. Tests of platelet function. *Curr. Opin. Hematol.* 14(5), 432–437 (2007).

115 Hagberg IA, Lyberg T. Blood platelet activation evaluated by flow cytometry: optimised methods for clinical studies. *Platelets* 11(3), 137–150 (2000).

116 Bluestein D. Research Approaches for Studying Flow Induced Thromboembolic Complications in Blood Recirculating Devices. *Expert Rev. Med. Devices* 1(1), 65–80 (2004).

117 Bluestein D. Towards optimization of the thrombogenic potential of blood recirculating cardiovascular devices using modeling approaches. *Expert Rev. Med. Devices* 3(3), 267–270 (2006).

Affiliations

- Gaurav Girdhar, PhD
  Department of Biomedical Engineering, State University of New York at Stony Brook, Stony Brook, NY, 11794-8181, USA
  Tel.: +1 631 444 1259
  Fax: +1 631 444 6646
  gaurav.girdhar@sunysb.edu
- Danny Bluestein, PhD
  Department of Biomedical Engineering, State University of New York at Stony Brook, Stony Brook, NY, 11794-8181, USA
  Tel.: +1 631 444 1259
  Fax: +1 631 444 6646
  danny.bluestein@sunysb.edu